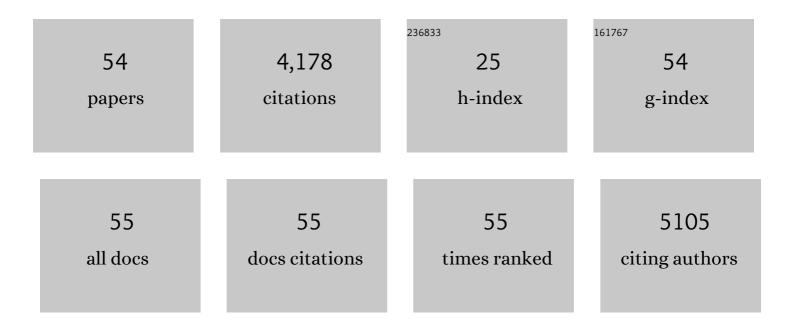
Weijiang Xue

List of Publications by Year in descending order

Source: https://exaly.com/author-pdf/3861027/publications.pdf Version: 2024-02-01



WEILANC XUE

#	Article	IF	CITATIONS
1	Acidâ€inâ€Clay Electrolyte for Wideâ€Temperatureâ€Range and Longâ€Cycle Proton Batteries. Advanced Materials, 2022, 34, e2202063.	11.1	16
2	Lithium Manganese Spinel Cathodes for Lithiumâ€lon Batteries. Advanced Energy Materials, 2021, 11, 2000997.	10.2	177
3	Ultra-high-voltage Ni-rich layered cathodes in practical Li metal batteries enabled by a sulfonamide-based electrolyte. Nature Energy, 2021, 6, 495-505.	19.8	323
4	Self-Perpetuating Carbon Foam Microwave Plasma Conversion of Hydrocarbon Wastes into Useful Fuels and Chemicals. Environmental Science & amp; Technology, 2021, 55, 6239-6247.	4.6	34
5	Dense Allâ€Electrochemâ€Active Electrodes for Allâ€Solidâ€State Lithium Batteries. Advanced Materials, 2021, 33, e2008723.	11.1	26
6	Thermally Aged Li–Mn–O Cathode with Stabilized Hybrid Cation and Anion Redox. Nano Letters, 2021, 21, 4176-4184.	4.5	6
7	Lowâ€Đensity Fluorinated Silane Solvent Enhancing Deep Cycle Lithium–Sulfur Batteries' Lifetime. Advanced Materials, 2021, 33, e2102034.	11.1	39
8	Stabilizing electrode–electrolyte interfaces to realize high-voltage Li LiCoO ₂ batteries by a sulfonamide-based electrolyte. Energy and Environmental Science, 2021, 14, 6030-6040.	15.6	84
9	FSI-inspired solvent and "full fluorosulfonyl―electrolyte for 4 V class lithium-metal batteries. Energy and Environmental Science, 2020, 13, 212-220.	15.6	198
10	Fast Heat Transport Inside Lithium-Sulfur Batteries Promotes Their Safety and Electrochemical Performance. IScience, 2020, 23, 101576.	1.9	28
11	Sacrificial Poly(propylene carbonate) Membrane for Dispersing Nanoparticles and Preparing Artificial Solid Electrolyte Interphase on Li Metal Anode. ACS Applied Materials & Interfaces, 2020, 12, 27087-27094.	4.0	8
12	Gradient-morph LiCoO ₂ single crystals with stabilized energy density above 3400 W h L ^{â~'1} . Energy and Environmental Science, 2020, 13, 1865-1878.	15.6	118
13	Molar-volume asymmetry enabled low-frequency mechanical energy harvesting in electrochemical cells. Applied Energy, 2020, 273, 115230.	5.1	12
14	Three-Dimensional SiC/Holey-Graphene/Holey-MnO ₂ Architectures for Flexible Energy Storage with Superior Power and Energy Densities. ACS Applied Materials & Interfaces, 2020, 12, 32514-32525.	4.0	8
15	Li metal deposition and stripping in a solid-state battery via Coble creep. Nature, 2020, 578, 251-255.	13.7	333
16	Manipulating Sulfur Mobility Enables Advanced Li-S Batteries. Matter, 2019, 1, 1047-1060.	5.0	63
17	Intercalation-conversion hybrid cathodes enabling Li–S full-cell architectures with jointly superior gravimetric and volumetric energy densities. Nature Energy, 2019, 4, 374-382.	19.8	449
18	Gradient Li-rich oxide cathode particles immunized against oxygen release by a molten salt treatment. Nature Energy, 2019, 4, 1049-1058.	19.8	248

WEIJIANG XUE

#	Article	IF	CITATIONS
19	Moderately concentrated electrolyte improves solid–electrolyte interphase and sodium storage performance of hard carbon. Energy Storage Materials, 2019, 16, 146-154.	9.5	73
20	Fluorine-donating electrolytes enable highly reversible 5-V-class Li metal batteries. Proceedings of the National Academy of Sciences of the United States of America, 2018, 115, 1156-1161.	3.3	512
21	Self-healing SEI enables full-cell cycling of a silicon-majority anode with a coulombic efficiency exceeding 99.9%. Energy and Environmental Science, 2017, 10, 580-592.	15.6	421
22	Double-oxide sulfur host for advanced lithium-sulfur batteries. Nano Energy, 2017, 38, 12-18.	8.2	93
23	Gravimetric and volumetric energy densities of lithium-sulfur batteries. Current Opinion in Electrochemistry, 2017, 6, 92-99.	2.5	100
24	<i>Ad hoc</i> solid electrolyte on acidized carbon nanotube paper improves cycle life of lithium–sulfur batteries. Energy and Environmental Science, 2017, 10, 2544-2551.	15.6	82
25	Nitrogen-Doped Carbon for Sodium-Ion Battery Anode by Self-Etching and Graphitization of Bimetallic MOF-Based Composite. CheM, 2017, 3, 152-163.	5.8	228
26	Si3N4-SiCw composites as structural materials for cryogenic application. Journal of the European Ceramic Society, 2016, 36, 2667-2672.	2.8	17
27	A novel processing route to develop alumina matrix nanocompositesreinforced with multi-walled carbon nanotubes. Materials Research Bulletin, 2015, 64, 323-326.	2.7	12
28	Sintering of Highâ€Performance Silicon Nitride Ceramics Under Vibratory Pressure. Journal of the American Ceramic Society, 2015, 98, 698-701.	1.9	37
29	Fracture toughness of 3mol% yttria-stabilized zirconia at cryogenic temperatures. Ceramics International, 2015, 41, 3888-3895.	2.3	4
30	Spark plasma sintering and characterization of 2Y-TZP ceramics. Ceramics International, 2015, 41, 4829-4835.	2.3	14
31	How Does Crack Bridging Change at Cryogenic Temperatures?. Journal of the American Ceramic Society, 2015, 98, 898-901.	1.9	6
32	Microstructure and mechanical properties of zirconia ceramics consolidated by a novel oscillatory pressure sintering. Ceramics International, 2015, 41, 10281-10286.	2.3	24
33	Crack propagation in silicon nitride ceramics under various temperatures and grain boundary toughness. Materials Science & Engineering A: Structural Materials: Properties, Microstructure and Processing, 2015, 632, 58-61.	2.6	10
34	Slow crack growth behavior of 3Y-TZP in cryogenic environment using dynamic fatigue and indentation technique. Materials Science & Engineering A: Structural Materials: Properties, Microstructure and Processing, 2015, 636, 203-206.	2.6	4
35	Mechanical and electrical properties of chemically modified MWCNTs/3Y-TZP composites. Ceramics International, 2015, 41, 9157-9162.	2.3	9
36	How does pore-induced crack change as temperatures decrease from 293 K to 77 K?. Ceramics International, 2015, 41, 15246-15249.	2.3	2

WEIJIANG XUE

#	Article	IF	CITATIONS
37	Fracture mechanism of a fracture-resistant CNT/alumina nanocomposite at cryogenic temperature. Ceramics International, 2015, 41, 13908-13911.	2.3	3
38	Toughening effect of multiwall carbon nanotubes on 3Y-TZP zirconia ceramics at cryogenic temperatures. Ceramics International, 2015, 41, 1303-1307.	2.3	14
39	Porous Alumina Ceramics with Unidirectional Oriented Pores Fabricated by Ionotropic Process of Sodium Alginate. Wuji Cailiao Xuebao/Journal of Inorganic Materials, 2015, 30, 877.	0.6	6
40	Fracture toughness of aluminum nitride ceramics at cryogenic temperatures. Ceramics International, 2014, 40, 13715-13718.	2.3	3
41	Strengthening mechanism of aluminum nitride ceramics from 293 to 77K. Materials Letters, 2014, 119, 32-34.	1.3	8
42	The dependence of interlocking and laminated microstructure on toughness and hardness of β-SiC ceramics sintered at low temperature. Materials Science & Engineering A: Structural Materials: Properties, Microstructure and Processing, 2013, 586, 338-341.	2.6	10
43	Enhanced toughness and hardness at cryogenic temperatures of silicon carbide sintered by SPS. Materials Science & Engineering A: Structural Materials: Properties, Microstructure and Processing, 2013, 569, 13-17.	2.6	14
44	Zirconia-based nanocomposite toughened by functionalized multi-wall carbon nanotubes. Journal of Alloys and Compounds, 2013, 581, 452-458.	2.8	28
45	Critical grain size and fracture toughness of 2mol.% yttria-stabilized zirconia at ambient and cryogenic temperatures. Scripta Materialia, 2012, 67, 963-966.	2.6	20
46	Enhanced fracture toughness of silicon nitride ceramics at cryogenic temperatures. Scripta Materialia, 2012, 66, 891-894.	2.6	35
47	Al2O3 ceramics with well-oriented and hexagonally ordered pores: The formation of microstructures and the control of properties. Journal of the European Ceramic Society, 2012, 32, 3151-3159.	2.8	33
48	Densification and mechanical properties of TiC by SPS-effects of holding time, sintering temperature and pressure condition. Journal of the European Ceramic Society, 2012, 32, 3399-3406.	2.8	84
49	Preparation and Properties of Porous Alumina with Highly Ordered and Unidirectional Oriented Pores by a Selfâ€Organization Process. Journal of the American Ceramic Society, 2011, 94, 1978-1981.	1.9	14
50	<i>R</i> â€Curve Behavior of 3 <scp>Y</scp> â€ <scp>TZP</scp> at Cryogenic Temperatures. Journal of the American Ceramic Society, 2011, 94, 2775-2778.	1.9	23
51	Research into mechanical properties of reaction-bonded SiC composites at cryogenic temperatures. Materials Letters, 2011, 65, 3348-3350.	1.3	12
52	Mechanical and thermal properties of 99% and 92% alumina at cryogenic temperatures. Ceramics International, 2011, 37, 2165-2168.	2.3	24
53	Ordered Macro–Mesoporous ncâ€īiO ₂ Films by Sol–Gel Method Using Polystyrene Array and Triblock Copolymer Bitemplate. Journal of the American Ceramic Society, 2008, 91, 2676-2682.	1.9	27
54	GIAXD and XPS Characterization of <i>sp</i> ³ C Doped SiC Superhard Nanocomposite Film. Key Engineering Materials, 0, 512-515, 971-974.	0.4	0